Coulomb Scattering of 1 MeV Electrons in Aluminum Foils

CH. BERGER, G. KNOP, H. KOFINK, D. MENZE, and W. SCHULZ

Physikalisches Institut der Universität Bonn

Received March 9, 1970

Electrons of a kinetic energy of 1 MeV were used to measure the angular dependence of the scattering cross section in thin aluminum foils. After correction for multiple scattering the results were compared with theoretical calculations including the radiative corrections. The measurements were found to agree with theory within $\pm 1\%$.

I. Introduction

The Coulomb scattering cross section of fast electrons can be written as a product of the Rutherford cross section and a factor $R(E, \Theta, Z)$ which depends on the total energy E of the incoming electrons, the scattering angle Θ of the outgoing electrons and the charge Z of the target nucleus. $R(E, \Theta, Z)$ was first calculated by Mott[1], later on by McKinley and Feshbach[2], and Dogget and Spencer[3]. Several authors have investigated the scattering cross section for electrons with a kinetic energy T of the order of 1 MeV. V. d. Graaff et al.[4], and Bayard and Intema[5] find agreement with theory within the quoted errors, whereas the results of the other authors [6-9] are not consistent with the theoretical values. A recent discussion of these papers can be found in the book of Roy and Reed[10].

The deviations from theory cannot be explained by the influence of radiative corrections[11], because this effect amounts only to 3% for 1 MeV electrons. In order to prove the radiative corrections we have

1 Mott, N. F.: Proc. Roy. Soc. (London), Ser. A **124**, 426 (1929).
2 McKinley, W. A. Jr., Feshbach, H.: Phys. Rev. **74**, 1759 (1948).
3 Dogget, J. A., Spencer, L. V.: Phys. Rev. **103**, 1597 (1956).
4 Graaff, R. J. V. d., Buechner, W. W., Feshbach, H.: Phys. Rev. **69**, 452 (1946).
5 Bayard, R. T., Intema, J. L.: Phys. Rev. **97**, 372 (1955).
6 Bothe, W., Kinzinger, E.: Z. Naturforsch. 7a, 390 (1952).
7 Paul, W., Reich, H.: Z. Physik **131**, 326 (1952).
8 Spiegel, V., Jr., Ruane, T. F., Anthony, D. J., Waldman, B., Miller, W. C.: Ann. of Physics 6, 70 (1959).
9 Rester, D. H., Rainwater, W. J.: Phys. Rev. **138**, A 12; **140**, A 165 (1965).
10 Roy, R. R., Reed, R. D.: Interactions of photons and leptons with matter. New York-London: Academic Press 1968.
11 Schwinger, J.: Phys. Rev. **76**, 790 (1949).

performed an experimental investigation of the scattering of 1 MeV electrons in thin aluminum foils for angles from 15 to 160 degree.

Since the radiative corrections are smaller than 3%, it is rather hopeless to determine them by absolute cross section measurement. On the other hand, it is well known, that they are zero at forward direction. Therefore our aim has been to improve the relative cross section measurements.

II. Coulomb Scattering and Corrections

a) Coulomb Scattering

The differential scattering cross section for electrons is given by

$$\frac{d\sigma}{d\Omega} = \sigma_R \cdot R(E, \Theta, Z) \tag{1}$$

where the symbols are defined as above.

The Rutherford cross section σ_R can be expressed as

$$\sigma_R = \frac{1}{4} Z^2 \cdot r_0^2 \frac{\gamma^2}{(\gamma^2 - 1)^2} \cdot \frac{1}{\sin^4 \Theta/2} \tag{2}$$

where

$$r_0 = e^2/m\,c^2, \qquad \gamma = E/m\,c^2$$

with e and m as the electron charge respective mass.

Z = 13
Kin. energy T = 1 MeV
E = T + $m_0 c^2$ = 1.51 MeV

R(θ) - R_1(θ) according to Dogget and Spencer

R(θ) - R_1(θ) according to Mc Kinley and Freshbach

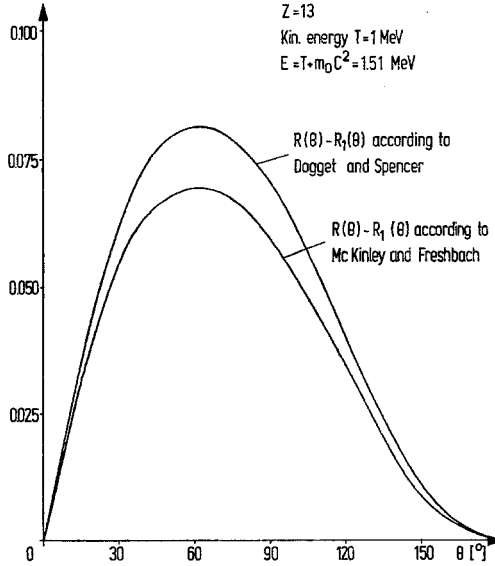Fig. 1. $R(E, \theta, Z)$-$R_1(E, \theta, Z)$ due to various approximations

$R(E, \Theta, Z)$ can be expanded in powers of $Z \cdot \alpha$, where α is the fine structure constant. The first term in the expansion (Born term or one photon exchange term) is given by the well known Mott formula [1]

$$R_1 = 1 - \beta^2 \sin^2 \Theta / 2 \qquad (3)$$

with $\beta = v/c$, and the second term [2] by

$$R_2 = \alpha Z \pi \beta \sin \Theta / 2 (1 - \sin \Theta / 2) \qquad (4)$$

Dogget and Spencer calculated the series numerically up to the 50th order. In Fig. 1 for $E = 1.5$ MeV and $Z = 13$ the deviation $R(E, \Theta, Z) - R_1(E, \Theta, Z)$ from the Mott term is shown according to various approximations.
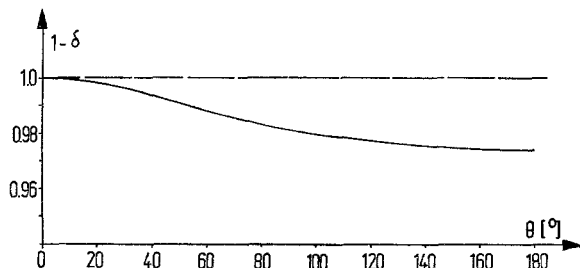
b) Radiative Corrections

The radiative corrections to the elastic scattering process due to real and virtual photons were first calculated by Schwinger [11]. Including the radiative correction, the experimentally observable cross section can be written as

$$\frac{d\sigma}{d\Omega} = \left(\frac{d\sigma}{d\Omega}\right)_{\text{Coul}} [1 - \delta(E, \varDelta E, \Theta)] . \qquad (5)$$

The main feature of the term δ is the logarithmic dependence on the energy resolution $\varDelta E$ of the detecting system:

$$\delta \sim \ln \frac{m}{\varDelta E} .$$

In Fig. 2 $(1 - \delta)$ is shown for $E = 1.51$ MeV, and $\varDelta E = 100$ keV.

RADIATIVE CORRECTION 1-δ ACCORDING TO SCHWINGER FOR ELECTRONS

Fig. 2. Radiative correction for electrons of a total energy $E = 1.51$ MeV and for $Z = 13$

c) Screening Effects

Formula (1) is derived under the assumption that the target nucleus is infinite heavy and unscreened. The modification of the Coulomb field due to the presence of atomic electrons can be treated in a simple way on the basis of the Thomas-Fermi model. We have estimated the screening effect to be negligible for $Z=13$ and $T=1$ MeV. The influence of the nuclear form factor was calculated due to a formula given by Rose[12]. The result is that the correction term is smaller than 0.1 % for $Z=13$ and $T=1$ MeV.

d) Electron-Electron Scattering

The only process which in concurrence to the electron-nucleon-interaction leads to a large angle scattering is the electron-electron collision. Due to the two body kinematics, the energy loss of the scattered electron is related to the scattering angle. Therefore — e. g. with the help of a magnetic-spectrometer — the electron-electron scattering can be separated kinematically from electron-nucleon scattering.

e) Multiple Scattering

Hitherto we have assumed all measured electron deflections to be the result of a single scattering of the electron. This is correct as far as the deflection angle is sufficient large and the foil thickness is sufficient small. In principle, the influence of plural and multiple scattering can be investigated experimentally by using foils of various thickness d and extrapolating to thickness zero. We have only used foils with ρd below 0.5 mg/cm². Herein ρ is the density. We made the extrapolation according to the theoretical work of Wegener[13]. In this paper the effect is divided into two parts: 1. a small angle multiple scattering, which is dominant at small scattering angles, 2. large angle dual scattering which is dominant at large scattering angles. The whole calculation is done for a foil perpendicular to the incoming beam.

III. Experimental Method

a) General Description

The counting rate is given by

$$N(\Theta, E, \Delta E) = N_{in} \, n_0 \, d \, \frac{d\sigma}{d\Omega} \, \Delta\Omega \tag{6}$$

where N_{in} is the number of incoming electrons, n_0 the number of target nuclei/cm³, d the foil thickness, and $\Delta\Omega$ the solid angle of the apparatus.

12 Rose, M. E.: Phys. Rev. 73, 279 (1948).
13 Wegener, H.: Z. Physik 351, 252 (1958).

To separate the influence of the radiative correction, one has to keep the overall experimental error below 1%, because the maximum value of δ is of the order 3%.

In order to avoid the difficulties of an absolute determination of the quantities d, $\Delta\Omega$ and N_{in} within the claimed accuracy, we have measured the cross sections relative to the cross section at a fixed angle Θ_0 (with $\sigma := d\sigma/d\Omega$)

$$S_{exp} = \frac{\sigma(\Theta, E, \Delta E)}{\sigma(\Theta_0, E, \Delta E)}. \tag{7}$$

A comparison of S_{exp} with the theoretical

$$S_{th} = \frac{\sigma_{coul}(\Theta, E)(1 - \delta(E, \Delta E, \Theta))}{\sigma_{coul}(\Theta_0, E)(1 - \delta(E, \Delta E, \Theta_0))} \tag{8}$$

shows any angular dependent deviation from the theory.

In such an experiment only the quantities Θ, E, ΔE must be determined absolutely.

The main problem is the measurement of the scattering angle Θ. Because of the strong angular dependence of the cross section $\sigma \sim 1/\sin^4(\Theta/2)$ a small error in Θ effects a large error in σ (e.g. at $\Theta = 30°$ $\Delta\Theta = 1.3 \cdot 10^{-4}$ causes $\Delta\sigma/\sigma = 10^{-3}$). Therefore a very accurate graduated circle for measuring the scattering angle is required, and furthermore the incoming beam has to be adjusted extremely carefully on the center of the graduated circle. If we choose the radius of the instrument to be 20 cm, the deviation from the center must not exceed 0.02 cm. Such an error is already induced by the influence of the earth magnetic field. In a magnetic field of 0.5 Gauß an electron with a kinetic energy of 1 MeV describes a circle with a radius of 100 m. Therefore the deviation from the straight line is 0.02 cm at a path length of 20 cm.

To overcome these difficulties, we have measured the scattering on the right as well as on the left side of the incoming beam. The principle is shown in Fig. 3. The curved incoming beam passes the center of the graduated circle at a distance h and the exit at a distance Δx from the ideal straight line. If we measure the counting rates $N_l(\tilde{\Theta})$ on the left side and $N_r(\tilde{\Theta})$ on the right side, the mean value is related to the ideal value $N(\Theta)$ by

$$\bar{N}(\Theta) = \tfrac{1}{2}[N_r(\tilde{\Theta}) + N_l(\tilde{\Theta})] = N(\Theta)(1 + K_1 + K_2). \tag{9}$$

K_1 is related to the uncertainty Δx. It can be shown that K_1 remains $< 10^{-3}$ if Δx does not exceed 0.08 cm.
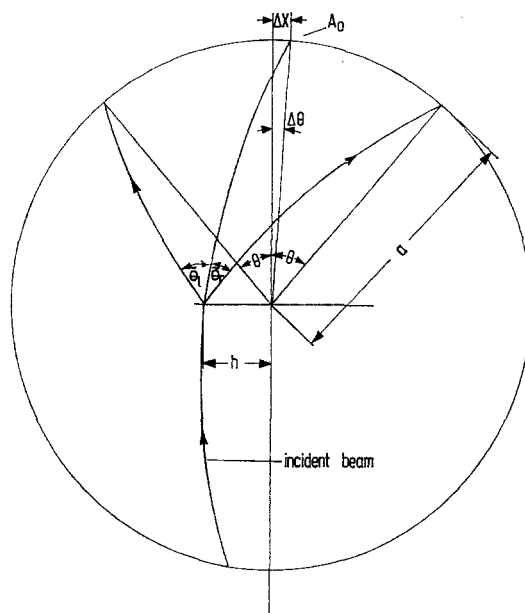
Fig. 3. Principle of determination of the scattering angle

K_2 is due to the uncertainty h and the curvature of the beam. The maximum value of K_2 is of the order of

$$K_{2_{max}} \approx 3 \left(\frac{h}{a} \right)^2.$$

This results in e. g. $K_{2\,max} \approx 10^{-3}$ for $h = 1$ cm and $a = 20$ cm.

In a similar way the error due to the eccentricity g of the scattering foil (Fig. 4) is reduced by measuring first in position 1, and after turning the foil by 180° in position 2. The mean value of these measurements is set to $N_r(\tilde{\Theta})$ respectively $N_l(\tilde{\Theta})$.

During the whole set of measurements the position of the scattering foil was choosen to be perpendicular to the incoming beam. Thus all additional uncertainties due to the determination of an effective foil thickness, e. g. if the foil is at an angle $\Theta/2$ respective to the incoming beam, were avoided. Of course, in this manner we could not measure the cross section at $\Theta = 90°$.

Our conclusion is that the method described above enables us to keep the strong angular dependent errors in the order of $0.2-0.3\%$, if the graduated circle allows to measure angles within an error of $\pm 5 \cdot 10^{-3}$ degree.
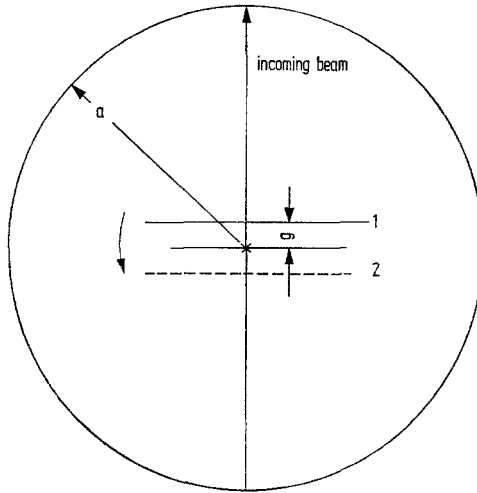
Fig. 4. Foil position

b) The Apparatus

The electrons are generated by a 1 MeV Van de Graaff accelerator (Fig. 5). Two horizontally deflecting magnets *M1*, *M3* and two vertically deflecting magnets *M2*, *M4* in connection with two horizontal slits *S1*, *S3* and two vertical slits *S2*, *S4* serve for adjusting fluctuations in the direction of the electron beam. The electron currents on the slits regulate the excitation of the magnet coils in such a way that the intensity behind the system has a maximum.

S3 is horizontally imaged by the magnet *M5* on the slit *S5*. *M5* is a sector magnet with 40° deflection angle and homogeneous field. It serves to keep the energy of the electrons constant by controlling the voltage of the Van de Graaff accelerator through the electron current on *S5*.
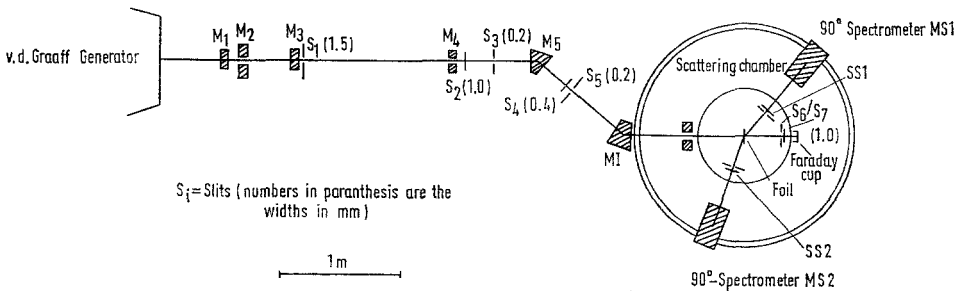

Fig. 5. Planview of the apparatus

A variation of $5 \cdot 10^{-4}$ in the magnetic field induces an error of 10^{-3} in the measured cross sections. Therefore we need a long time stability of $5 \cdot 10^{-4}$ during the runs. The simplest way to achieve this is to use an aged permanent magnet.

For the absolute determination of the electron energy we measured the electron diffraction patterns behind a thin aluminum foil (thickness: $8 \cdot 10^{-2}$ mg/cm^2). The result for the kinetic energy of the electron was

$$T = 990 \pm 4 \text{ keV}.$$

The resulting maximum error in σ is 0.5% at $\Theta = 160°$.

Before entering the scattering chamber the electrons pass the magnetic inflector *MI*. This magnet is needed to direct the beam on the center of the foil and to reduce the influence of the stray field of spectrometer *MS*1 and *MS*2. The inflector is a sector magnet with 40° deflection angle and homogeneous field. In horizontal direction the magnet focuses the beam on the scattering foil. To get a weak vertical focusing we used the edge effect with an exit and entry angle of 10.5° with respect to the normal on the pole faces. With the help of additional coils on the magnet poles the position of the electron beam has been controlled to be at the center of the slit *S6* at the exit of the scattering chamber. The electrons are stopped in a small Faraday cup in order to control the intensity of the accelerator. The mean intensity of the incoming beam was 10^{-9} A. The beam size on the foil was about 0.3×0.3 mm.

The scattering chamber itself was made out of stainless steel, and had a diameter of 600 mm and a height of 550 mm. The chamber had exits at 0° and 180° and at 15°, 30°, 50°, 70°, 90°, 110°, 130°, 145°, 160° as well on the right as on the left side. In the center of the chamber the graduated circle was adjusted with an accuracy of 0.1 mm in all directions. The instrument had a diameter of 400 mm and was proved to have an accuracy of $\pm 4 \cdot 10^{-3}$ degree at all angles. The scattering foil could be adjusted at the center of the graduated circle with an eccentricity of 0.1 mm. The solid angle of 0.018 msr for the scattered electrons was defined by a pair of crossed slits (*SS1*, *SS2*) at each side, mounted on arms which can rotate around the pivot.

The scattered electrons were focused on the exit slits of two completely identical magnetic spectrometers *MS1* and *MS2*. Each spectrometer consisted of a sector magnet (homogeneous field) with a deflection angle of 90° and a sector angle of 40° giving a focusing in radial and axial direction due to edge effect. The scattered electrons are deflected in the vertical plane. This is advantageous with respect to the dimensions of the apparatus and to the shielding of the scintillation counters against the background radiation. The radius of the mean orbit is 20 cm at a

magnetic field of 230 Gauß. The dispersion $\Delta x/\Delta E$ amounts to 0.43 mm/keV. The entry and exit angle is 25°.

The exit slit of the spectrometer had a width of 40 mm and was mounted along the radial image plane. Electrons with an energy loss $\Delta E < 97$ keV could pass the exit slit and were detected by a scintillation counter (plastic scintillator and RCA 6810 photomultiplier). Electrons which made an electron-electron collision are rejected, because even at $\Theta = 15°$ the energy loss of those electrons is 140 keV. On the other hand with $\Delta E \approx 100$ keV we are sure to count all elastically scattered electrons.

The scintillator and the photomultiplier were shielded against the γ-ray background of the laboratory with a 10 cm thick lead-cylinder. The only remaining background was due to cosmic rays and thermal noise of the multiplier. It was about 2% of the counting rate at $\Theta = 160°$. RCA 6810 photomultiplier were choosen because they were proved to have a very low long-time gain drift [14].

The pulses were shaped by fast discriminators and counted by 10 MHZ scalers (Fa. Borer, Solothurn, Switzerland). The scalers were only gated when the current in the Faraday-cup exceeded 10^{-10} A. Typical counting rates were $4 \cdot 10^4$/sec at $\Theta = 15°$ and a foil thickness of 0.5 mg/cm², and 1/sec at $\Theta = 160°$ and a foil thickness of 0.25 mg/cm².

Both spectrometers were mounted on racks which could be turned easily round the axis of the scattering chamber. In the whole system from the cathode of the Van de Graaff accelerator down to the plastic scintillators, a vacuum of 2×10^{-5} Torr was hold by three oil diffusion pumps.

IV. Data Analysis

We define $N_l(\Theta, 1)$ to be the counting rate at an angle Θ on the "left side", where the solid angle $\Delta\Omega_1$ is defined by the slit $SS1$. All counting rates on the left side were measured with spectrometer $MS1$, whereas all counting rates on the right side were measured with spectrometer $MS2$. At 15°, 30°, 50°, 70°, 110°, 130° on the left side, we have measured the counting rates $N_l(\Theta, 1)$ versus the rates $N_r(\Theta_0, 2)$ (measured with spectrometer $MS2$ at a fixed angle Θ_0, where $\Delta\Omega_2$ is defined by the slit $SS2$) for both foil positions, and have calculated the ratios

$$R_1 = \frac{N_l(\Theta, 1)}{N_r(\Theta_0, 2)}. \tag{10}$$

The averaging over the different counting rates respective to foil position 1 or 2 (see Fig. 5) is yet included.

---

14 Kofink, H.: Diplomarbeit Bonn 1965, unpublished.

In a similar way we measured

$$R_2 = \frac{N_r(\Theta, 1)}{N_l(\Theta_0, 2)}. \tag{11}$$

The fixed angle Θ_0 has been choosen to $50°$.

For the comparison of the counting rates to the theoretical values the ratios

$$a = \frac{N_r(\Theta_0, 1)}{N_l(\Theta_0, 2)} \tag{12}$$

and

$$b = \frac{N_r(\Theta_0, 2)}{N_l(\Theta_0, 1)} \tag{13}$$

are needed, as is shown below.

These ratios are only determined by the angular asymmetry of the apparatus at the fixed angle Θ_0 and by the ratio of the solid angles $\Delta\Omega_1$ and $\Delta\Omega_2$ defined by the slits $SS1$ and $SS2$:

$$a = (1+\varepsilon)\frac{\Delta\Omega_1}{\Delta\Omega_2}, \tag{14}$$

$$b = (1+\varepsilon)\frac{\Delta\Omega_2}{\Delta\Omega_1} \tag{15}$$

where $1+\varepsilon$ can be expressed by the asymmetry

$$1+\varepsilon = \frac{N_r(\Theta_0, 1)}{N_l(\Theta_0, 1)} = \frac{N_r(\Theta_0, 2)}{N_l(\Theta_0, 2)} \tag{16}$$

$(1+\varepsilon)$ cannot be measured directly but calculated with the help of the measured ratios a and b

$$1+\varepsilon = \sqrt{ab}. \tag{17}$$

For evaluation of the relative shape of the cross section we must relate all counting rates to the average counting rate

$$N_0 = \tfrac{1}{2}\left(N_r(\Theta_0, 1) + N_l(\Theta_0, 1)\right) = N_r(\Theta_0, 1)\left(1 - \frac{\varepsilon}{2}\right). \tag{18}$$

We have

$$\frac{N_r(\Theta, 1)}{N_0} = \frac{R_2}{a}\left(1 + \frac{\varepsilon}{2}\right) \tag{19}$$

Table 1. *Measured counting rates*

θ (°)	$\dfrac{N_l(\theta, 1)}{N_0}$	$\dfrac{N_r(\theta, 1)}{N_0}$	$\dfrac{1}{2}\left(\dfrac{N_l}{N_0}+\dfrac{N_r}{N_0}\right)$	$\rho \cdot d$ (mg/cm²)	Error (%)
15	125.00	120.31	122.66	0.1	
	125.80	121.58	123.68	0.25	0.41
	125.97	121.41	123.69	0.5	
30	8.045	7.592	7.819	0.1	
	8.022	7.629	7.826	0.25	0.32
	8.013	7.646	7.830	0.5	
50	1.011	0.989	1.000	0.1	
	1.011	0.989	1.000	0.25	0.30
	1.011	0.989	1.000	0.5	
70	$2.532 \cdot 10^{-1}$	$2.503 \cdot 10^{-1}$	$2.518 \cdot 10^{-1}$	0.1	
	$2.545 \cdot 10^{-1}$	$2.509 \cdot 10^{-1}$	$2.527 \cdot 10^{-1}$	0.25	0.30
	$2.549 \cdot 10^{-1}$	$2.502 \cdot 10^{-1}$	$2.526 \cdot 10^{-1}$	0.5	
110	$3.524 \cdot 10^{-2}$	$3.473 \cdot 10^{-2}$	$3.499 \cdot 10^{-2}$	0.1	
	$3.548 \cdot 10^{-2}$	$3.492 \cdot 10^{-2}$	$3.520 \cdot 10^{-2}$	0.25	0.47
	$3.564 \cdot 10^{-2}$	$3.542 \cdot 10^{-2}$	$3.553 \cdot 10^{-2}$	0.5	
130	$1.559 \cdot 10^{-2}$	$1.579 \cdot 10^{-2}$	$1.569 \cdot 10^{-2}$	0.1	
	$1.548 \cdot 10^{-2}$	$1.558 \cdot 10^{-2}$	$1.553 \cdot 10^{-2}$	0.25	0.62
	$1.562 \cdot 10^{-2}$	$1.556 \cdot 10^{-2}$	$1.559 \cdot 10^{-2}$	0.5	
145	$8.78 \cdot 10^{-3}$	$8.78 \cdot 10^{-3}$	$8.78 \cdot 10^{-3}$	0.25	0.90
160	—	$5.33 \cdot 10^{-3}$	$5.33 \cdot 10^{-3}$	0.25	0.80

which follows from (11) and (12), and with the help of (10), (13), (16) and (17) we can calculate

$$\frac{N_l(\Theta, 1)}{N_0} = R_1 \cdot b \cdot \left(1 - \frac{\varepsilon}{2}\right). \tag{20}$$

These ratios give us the relative shape of the cross section.

We have measured the cross section for aluminum-foils. This procedure was done for three foils of different thickness. In Table 1 the result of the left side and right side measurements and the mean values of both are listed for the various foil thicknesses. The quoted errors are due to the mean values of N/N_0 and include quadratic addition of the statistical error and the error due to background subtraction [15].

In order to correct for multiple scattering the mean relative counting rate versus the foil thickness was plotted for each scattering angle. The ratio is given by

$$\frac{\overline{N}}{N_0} = \frac{\sigma}{\sigma_0}(1 + \alpha \rho d) \tag{21}$$
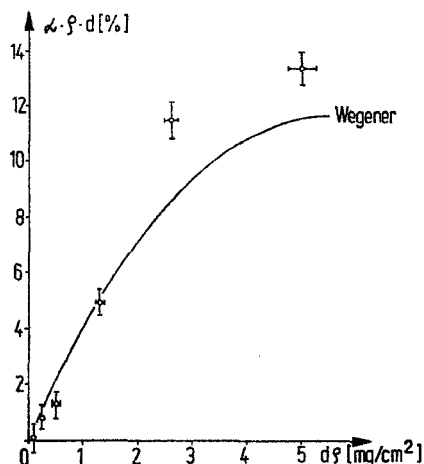
---

15 Schulz, W.: Diplomarbeit Bonn 1967, unpublished.

Fig. 6. Multiple scattering effect for $\theta = 110°$ versus thickness of scattering foil

because of the normalization to N_0 and formula (6). The straight lines through the points were fitted with the coefficient α calculated according to Wegener[12]. Thus we got the relative cross section σ/σ_0 at zero foil thickness. To prove this procedure we extended at $\theta = 110°$ the measurements to ρd values of 5 mg/cm². The result is shown in Fig. 6 where $\alpha \rho d$ is plotted versus ρd for $\theta = 110°$. The agreement with the theoretical model is quite good.

For $\theta = 50°$ we found no measurable effect within the statistical error. This is in agreement with the prediction of Wegener, who calculated a minimum of the influence of multiple scattering at $\theta \approx 50°$.

At $\theta = 145°$, we only have one measurement for $\rho d = 0.25$ mg/cm² and at $\theta = 160°$ we must even omit the "left side" measurement, because the time needed to do the whole set of measurements grew to high. On the other hand, the extrapolating procedure was extensively proved at smaller angles. At $\theta = 160°$ the influence of the asymmetry of the apparatus becomes very small.

V. Results and Discussion

In Table 2 (column 2, 3) the extrapolated cross sections at zero foil thickness

$$S_{\text{exp}} = \frac{\sigma(\theta)}{\sigma_0}$$

are listed together with their estimated errors. In addition to the errors quoted in Table 2, the errors due to the determination of the energy

Table 2. *Final Results*

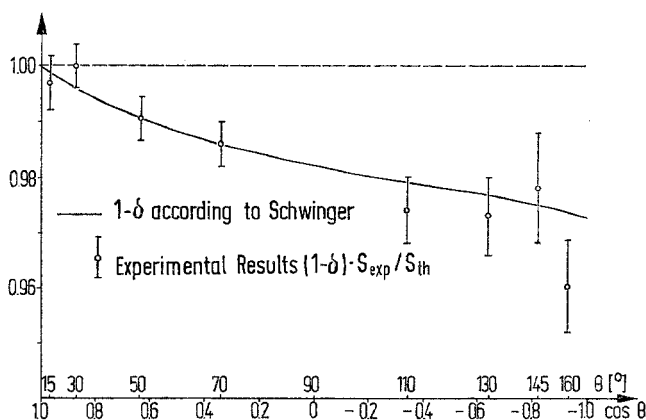| θ ($°$)	$\left(\dfrac{\sigma}{\sigma_0}\right)_{\exp}$	Error (%)	$\left(\dfrac{\sigma}{\sigma_0}\right)_{\text{coul}} \dfrac{1-\delta}{1-\delta_0}$	$\dfrac{S_{\exp}}{S_{\text{th}}}(1-\delta)$	$1-\delta$
0	—	—	—	—	1.000
15	122.73	0.87	122.98	0.997	0.999
30	7.819	0.40	7.785	1.000	0.996
50	1.000	0.39	1.000	0.991	0.991
70	$2.140 \cdot 10^{-1}$	0.39	$2.514 \cdot 10^{-1}$	0.986	0.986
110	$3.488 \cdot 10^{-2}$	0.61	$3.513 \cdot 10^{-1}$	0.972	0.979
130	$1.548 \cdot 10^{-2}$	0.74	$1.552 \cdot 10^{-2}$	0.974	0.977
145	$8.78 \ \cdot 10^{-3}$	1.1	$8.76 \ \cdot 10^{-3}$	0.978	0.975
160	$5.33 \ \cdot 10^{-3}$	1.1	$5.40 \ \cdot 10^{-3}$	0.960	0.974

Fig. 7. Comparison between the experimental results and theory

and the scattering angle of the electrons are quadratically added. For $\Theta = 145°$ and $160°$ we estimated an additional error of 0.5% because of the missing extrapolation procedure. The error due to the missing left side measurement is negligible at $\Theta = 160°$.

In the fourth column of Table 2 the relative dependence of the theoretical cross section

$$S_{\text{th}} = \frac{\sigma_{\text{coul}}(\Theta)(1-\delta)}{\sigma_{\text{coul}}(\Theta_0)(1-\delta_0)}$$

is given, where σ_{coul} was calculated according to Dogget and Spencer[3] and $(1-\delta)$ according to Schwinger[11]. To evaluate the measured dependence of the radiative corrections we plotted $(S_{\exp}/S_{\text{th}})(1-\delta)$ (Table 2, column 5) versus $\cos \Theta$ (Fig. 7). The solid curve is given by $(1-\delta)$. The agreement of the experimental points with theory is very good,

and the influence of the radiative corrections is shown very clear. We found $\chi^2 = 4, 3$ for 7 degrees of freedom. On the other hand, the χ^2 value without the radiative correction is 64.

Dr. Christof Berger
Prof. Dr. G. Knop
Dipl.-Phys. Helga Kofink
Dipl.-Phys. Dietmar Menze
Dipl.-Phys. Winfried Schulz
Physikalisches Institut der Universität
D-5300 Bonn, Nussallee 12